8-2011

Differential expression of voltage-gated K+ currents in medial septum/diagonal band complex neurons exhibiting distinct firing phenotypes

Emilio R. Garrido-Sanabria

Miriam G. Perez-Cordova

Luis V. Colom
The University of Texas Rio Grande Valley

Recommended Citation

Garrido-Sanabria, E. R., Perez-Cordova, M. G., & Colom, L. V. (2011). Differential expression of voltage-gated K+ currents in medial septum/diagonal band complex neurons exhibiting distinct firing phenotypes. Neuroscience research, 70(4), 361–369. https://doi.org/10.1016/j.neures.2011.05.011

Published in final edited form as:
Neurosci Res. 2011 August ; 70(4): 361–369. doi:10.1016/j.neures.2011.05.011.

Differential expression of voltage-gated K^+ currents in medial septum/diagonal band complex neurons exhibiting distinct firing phenotypes

Emilio R. Garrido-Sanabria, **Miriam G. Perez-Cordova**, and **Luis V. Colom***
Department of Biological Sciences, The Center for Biomedical Studies, The University of Texas at Brownsville, 80 Fort Brown, Brownsville, Texas 78520

Abstract

The medial septum/diagonal band complex (MSDB) controls hippocampal excitability, rhythms and plastic processes. Medial septal neuronal populations display heterogeneous firing patterns. In addition, some of these populations degenerate during age-related disorders (e.g. cholinergic neurons). Thus, it is particularly important to examine the intrinsic properties of theses neurons in order to create new agents that effectively modulate hippocampal excitability and enhance memory processes. Here, we have examined the properties of voltage-gated, K^+ currents in electrophysiologically-identified neurons. These neurons were taken from young rat brain slices containing the MS/DB complex. Whole-cell, patch recordings of outward currents were obtained from slow firing, fast-spiking, regular-firing and burst-firing neurons. Slow firing neurons showed depolarization-activated K^+ current peaks and densities larger than in other neuronal subtypes. Slow firing total current exhibited an inactivating A-type current component that activates at subthreshold depolarization and was reliably blocked by high concentrations of 4-AP. In addition, slow firing neurons expressed a low-threshold delayed rectifier K^+ current component with slow inactivation and intermediate sensitivity to tetraethylamonium. Fast-spiking neurons exhibited the smaller I_K and I_A current densities. Burst and regular firing neurons displayed an intermediate firing phenotype with I_K and I_A current densities that were larger than the ones observed in fast-spiking neurons but smaller than the ones observed in slow-firing neurons. In addition, the prevalence of each current differed among electrophysiological groups with slow firing and regular firing neurons expressing mostly I_A and fast spiking and bursting neurons exhibiting mostly delayer rectifier K^+ currents with only minimal contributions of the I_A. The pharmacological or genetic modulations of these currents constitute an important target for the treatment of age-related disorders.

Keywords

cholinergic neurons; slow firing; fast-spiking; regular spiking; voltage-gated K^+ currents; firing properties; medial septum; rat

*Corresponding author: Luis V. Colom, MD, PhD., Dept. Biological Sciences, The University of Texas at Brownsville, 80 Fort Brown, Brownsville, TX 78520, Phone: (956) 882-5048, Fax: (956) 882-5043, luis.colom@utb.edu.

INTRODUCTION

The medial septum/diagonal band complex (MS/DB) plays a pivotal role in the synchronization of septohippocampal pathways, pacing oscillatory activity such as the theta rhythm (Andersen et al., 1979; Bland and Oddie, 2001; Bland et al., 1999; Bland and Bland, 1986; Jackson and Bland, 2006; Lawson and Bland, 1993). It is largely known that neurons in the MS/DB express diverse intrinsic membrane properties (*e.g.* firing pattern, action potential width, afterhyperpolarizing potentials and accommodation), which tend to correlate with their neurochemical phenotypes (*e.g.* neurotransmitter content) (Garrido-Sanabria et al., 2007b; Griffith, 1988; Griffith and Matthews, 1986; Knapp et al., 2000; Morris et al., 1999; Sotty et al., 2003). For instance, slow firing neurons are known to express markers of cholinergic neurons such as acetylcholinesterase, acetylcholine and nerve growth factor low-affinity receptor P75 (Garrido-Sanabria et al., 2007b; Griffith and Matthews, 1986; Sotty et al., 2003; Wu et al., 2003; Yoder and Pang, 2005). Typically, these neurons slow significantly in their firing afterhyperpolarizing potential (sAHP) and wide action potentials (Garrido-Sanabria et al., 2007b; Griffith and Matthews, 1986; Matthews and Lee, 1991; Sotty et al., 2003). In contrast, fast-spiking and burst firing neurons usually express L-glutamic acid decarboxylase (GAD) immunoreactivity, indicating that they are gamma-aminobutyric acid (GABA)ergic neurons (Knapp et al., 2000; Morris et al., 1999; Serafin et al., 1996; Sotty et al., 2003; Yoder and Pang, 2005). Among this group, parvalbumin-containing neurons have been extensively studied in the MS/DB area. Parvalbumin-positive neurons are characterized *in vitro* by their salient capability to fire short-duration action potentials at sustained high-frequency rates with little accommodation (Griffith, 1988; Knapp et al., 2000; Morris et al., 1999). The majority of parvalbumin-containing neurons project their axons toward the hippocampus as part of the septohippocampal pathway (Brauer et al., 1998; Freund, 1989; Kiss et al., 1990; Morris and Henderson, 2000).

Electrophysiologically, neurons in the medial septal region have been classified as slow-firing, fast-spiking, regular-spiking, and burst-firing neurons (Henderson et al., 2001). The emergence of such dissimilar firing phenotypes depends on the interaction of different ionic currents. Among these currents, potassium (K^+) conductances are known to shape electrical properties of cells, influencing the duration and repolarization phase of action potentials, afterhyperpolarizing potentials and repetitive firing patterns (Li et al., 2006). Several types of K^+ channels have been identified based on their electrophysiological and pharmacological properties. The most widely distributed K^+ channels are the delayed outward rectifier (I_{DR}), transient A-type (I_A), and calcium-activated potassium (I_{KCa}) conductances (Coetzee et al., 1999; Rudy, 1999). The I_{DR} and I_A conductances regulate the timing of action potential formation and the repetitive firing pattern of neuronal cells (Hernandez-Pineda et al., 1999; Peusner et al., 1998; Schwindt et al., 1988; Song et al., 1998; Traub et al., 1991). Correlation between firing behavior and K^+ currents has previously been explored in the MS/DB. For example, apamin-sensitive Ca^{2+}-dependent K^+ currents underlying slow afterhyperpolarizing potentials (sAHP) have been described in slow firing cholinergic neurons of the MS/DB, and they are thought to contribute to the neurons' strong spike adaptation (Griffith, 1988; Griffith and Matthews, 1986; Matthews and Lee, 1991). In contrast, fast-spiking neurons exhibiting markedly fast afterhyperpolarizing potential (fAHP) and little accommodation express modest apamin-sensitive Ca^{2+}-dependent K^+ current (Morris et al., 1999; Sotty et al., 2003). Previous experiments in striatum have revealed that cholinergic neurons are able to fire at low frequencies due to the presence of a pronounced A-type K^+ current, which is mainly mediated via Kv 4.2 channels (Song et al., 1998; Tkatch et al., 2000). However, a comparative study on major types of K^+ currents has not been performed among neurons with distinct firing repertoires in the MS/DB.

The septo-hippocampal system is affected by aging and Alzheimer's disease (Geula, 1998; Hall et al., 2008; Schliebs and Arendt, 2006). Medial septal neurons act as pacemakers for the hippocampal theta rhythm, a functional state that enhance synaptic plasticity and memory processes (Colom, 2006). The rhythmical firing patterns of medial septal neurons are dependent on their intrinsic membrane properties. In turn, intrinsic membrane properties are shaped by ionic conductances. K^+ channels constitute the largest family of membrane ionic channels. Their extraordinary diversity makes them a perfect tool to control neuronal excitability and firing properties. Some K^+ channels, such as the $K_v3.1$ of medial septal GABAergic neurons may contribute to hippocampal theta activity through the regulation of transmitter release from axonal terminals (Henderson et al., 2010). Furthermore, I_{KD} and I_A currents have been associated with Alzheimer's disease pathogenesis, contributing to brain dysfunction and cell death mechanisms (Angulo et al., 2004; Colom et al., 1998; Kerrigan et al., 2008; Kidd et al., 2006; Kidd and Sattelle, 2006; Pannaccione et al., 2007; Plant et al., 2006; Ye et al., 2003; Yu et al., 2006). Thus, the characterization of K^+ currents in medial septal neurons is necessary to understand the septo-hippocampal function as well as devastating disorders such as Alzheimer's disease.

Here, we explore the properties of voltage-gated K^+ currents that can determine distinct discharge patterns in electrophysiologically-identified neurons in the MS/DB area. In this study, we have used the whole-cell, patch-clamp technique to examine the voltage-gated K^+ currents that participate in the generation of the firing patterns of MS/DB neurons. Our results suggest that physiologically defined neuron subtypes display diverse voltage-gated K^+ currents, which actively contribute to shaping the action potential waveforms, spike frequency and excitability of MS/DB neurons.

MATERIALS AND METHODS

Medial septum/diagonal band complex preparations

Animal protocols used in this study complied with pertinent institutional and federal animal welfare regulations (Protocol#2003-004-IACUC). Electrophysiological experiments were performed using the coronal MS/DB slice preparation. 35, male, Sprague Dawley rats (21–35 days old; Charles River Laboratories, Raleigh, NC) were deeply anesthetized with 80 mg/kg ketamine i.p. (Butler Animal Health Supply, Dublin, OH) and decapitated with a rodent guillotine. The brain was rapidly removed and placed into ice-cold (~4°C) sucrose-artificial cerebrospinal fluid (ACSF) containing (in mM): 240 sucrose, 3 KCl, 1 $CaCl_2$, 5 $MgSO_4$, 0.15 NaH_2PO_4, 26 $NaHCO_3$, 25 glucose, pH 7.4 following aeration with 95% O_2 and 5% CO_2; osmolarity was 295–305 mOsm as measured with a freezing point osmometer (Advanced Instruments; Needham, MA). The block was glued to the stage of a vibrating tissue slicer (OTS-4000, EMS, Fort Washington, PA), and coronal slices of the MS/DB area (350 μm) were sectioned in ice-cold, oxygenated ACSF. Slices were allowed to recover in a holding chamber containing oxygenated standard ACSF (see below) for 1–2 hours at room temperature until needed.

For recording, individual slices were transferred to a slice chamber, which was fixed to the stage of an upright microscope (Axioskop; Zeiss, Oberkochen, Germany), fitted with a water immersion objective (40×, 0.75 numerical aperture) and viewed with near infrared light (>775 nm) trans illumination and differential interference contrast optics (IR-DIC). Slices were continuously perfused (at 1.5 ml min^{-1}) with ACSF containing (in mM):125 NaCl, 3 KCl, 2 $CaCl_2$, 2 $MgSO_4$, 5 BES, 15 D-glucose, aerated with 95 % O_2.5 % CO_2. All drugs were added into the perfusate by switching to reservoirs containing the appropriate test solution. A waiting period of ~10 min was used to allow for equilibration before data were collected.

Electrophysiology

Recordings were made from visually identified neurons in the MS/DB area. All neurons were initially identified on the basis of somata shapes using IR-DIC optics. Recording pipettes pulled in multiple stages on a Flaming-Brown P-97 horizontal puller (Sutter Instruments, Novato, CA) from borosilicate glass (1.5 mm ID), which had a resistance of 3 to 5 M . Patch electrodes were filled with a solution comprising the following (in mM): 120 K-gluconate, 10 KCl, 1 $MgCl_2$, 2.5 Mg-ATP, 10 HEPES, 0.25 Na_2-GTP, 0.1 BAPTA and 0.1% neurobiotin (pH 7.2 with KOH; 290 mOsm). The patch electrode was advanced towards a visualized neuron using a stepping micromanipulator (PMC 100, Newport; Irvine, CA). Once the pipette made contact with a cell, negative pressure was used to form a gigaohm (>1 GΩ) cell-pipette seal. Then, gentle suction was applied to rupture the patch membrane. Seal formation was performed in current-clamp mode, and membrane breakthrough was monitored by observing the response to a hyperpolarizing current step (0.3 nA).

Whole-cell patch-clamp techniques were used in current-clamp and voltage-clamp modes on the same cell. This was done to identify the voltage-gated K^+ currents present and to examine their contribution to the firing pattern of the cell. Neurons were first recorded in current-clamp mode for the analysis of intrinsic membrane properties (*e.g.* action potential shape and firing characteristics). This was done using the electronic "bridge" circuit of Axopatch 1D amplifier (Molecular Devices Corporation, Sunnyvale, CA) with the output filter set at 10 kHz. Signals were digitized with a DIGIDATA 1300A A/D board (Molecular Devices Corporation) and stored on PC running pClamp9 software (Molecular Devices Corporation). After completing the examination of action potential and firing patterns in current-clamp mode, we switched to the voltage-clamp configuration to record K^+ currents. Series and access resistance were monitored continually, and cells were discarded if access resistance was unstable or changed by more than 20%. Potentials were recorded with respect to the Ag/AgCl reference electrode located near the outflow of the chamber. Liquid junction potentials ~10 mV were estimated between the pipette and external solutions, but values of membrane potentials were not corrected.

Intrinsic properties were analyzed off-line using the Clampfit 9 program of pCLAMP9 software. The firing pattern was defined by the response of the cell to 400-ms increment depolarizing steps. Other parameters measured included resting membrane potential, input resistance, membrane time constant, action potential height, action potential half-width, rise slope and decay slope. The action potential threshold was defined as the lowest current injected that elicited an action potential with an overshoot. The frequency was calculated as the maximum number of action potentials elicited at the activation threshold. The action potential overshoot was determined from 0 mV to the peak of an action potential. The duration of the action potential was measured at 50% and 75% of the peak amplitude from the resting membrane potential. This was done because the 50% amplitude was close to the base of the action potential and the 75% amplitude was close to the inflection on the falling phase of the action potential (Stucky and Lewin, 1999) (Stucky and Lewin, 1999).

After assessing the intrinsic properties, neurons were voltage-clamped at −70 mV to study outward rectifier (I_K) and A-type K^+ currents (I_A). To selectively record K^+ currents and minimize the contributions from Ca^{2+} and Na^+ currents, the extracellular solution was replaced by a solution containing 1 μM tetrodotoxin (TTX, from Sigma-Aldrich, St. Louis, MO). Since Ca^{2+} currents were not easily eliminated even in the Ca^{2+} -free control solution in slice preparation, we replaced Ca^{2+} on an equimolar basis by Mg^{2+} and added 0.2–0.4 mM $CdCl_2$ to the ACSF solutions. In some experiments, tetraethylammonium chloride (TEA-Cl) or 4-aminopyridine (4-AP) was applied. When 4-AP was included in the ACSF, the pH was adjusted to 7.4 using H_2SO_4. When high concentrations (≥1 mM) of 4-AP or

TEA-Cl were added to the solution, the osmolarity was adjusted by reducing NaCl from the ACSF solutions.

Charge transfer densities for I_K and I_A currents were calculated to account for the small variations in cell size and inactivation kinetics. Current density was obtained by dividing the current amplitude by the cell capacitance, which was estimated by fitting the current induced by a small (10 mV) hyperpolarizing step. To activate voltage-gated K^+ currents, pre-designed protocols of depolarizing test pulses whereas a 100-ms hyperpolarizing prepulse (to −110 mV) was applied to maximally activate I_A as depicted in Figure 1. A conditioning pre-pulse (100-ms) of −50 mV was used to inactivate I_A to allow for trace subtraction and isolation of the A-type component from the total K^+ current. The voltage threshold for activation was determined as the voltage at which the upward inflections of the current traces start to occur when evoked via specific voltage step protocols for I_A and I_K. Linear leak currents, through membrane capacitance, were cancelled on-line using P/4 procedure in Pclamp 9.

Data were analyzed using the Clampfit 9 software program (PCLAMP9). Whole cell current-voltage (*I–V*) curves for individual neurons were generated by calculating the mean peak outward current at each testing potential and normalizing them for cell capacitance. The amplitude of the K^+ current was measured at the peak.

Data were fitted to the Boltzmann equation:

$$I=C+\{I_{max}/[1+exp(V_{1/2}-V_m/k)]\}$$

In this equation, $V_{0.5}$ is the membrane potential at which 50% of activation was observed; k is the slope of the function; C is a constant (= 0 in the *IV* relation); I_{max} is the maximal K^+ current density, and V_m is the membrane potential. 4-AP and TEA-sensitive K^+ currents were obtained by subtracting the 4-AP and TEA-resistant K^+ current from the total K^+ current. Concentration-response data were fitted according to the Hill relationship $\{I/I_{max} = 1/[1+(X)/IC_{50}]^n\}$. Data are presented as mean ± standard error of the mean (SEM or as mean ± standard deviation (SD). `Comparisons between means were tested for significance using paired and unpaired Student's *t*-test or one-way ANOVA with post-hoc comparisons by Tukey's Honest Statistical Difference (HSD); $P<0.05$ is considered statistically significant.

Chemicals

Tetradotoxin (TTX), 4-aminopyridine (4-AP), tetraethylamonium chloride (TEA-Cl) were purchased from Sigma-Aldrich Co, Saint Louis, USA.

RESULTS

A-type, K^+ current density is expressed differentially among MS/DB neurons with distinct firing phenotypes

Neurons in the MS/DB area exhibit a distinct firing repertoire, suggesting possible differences in the expression of voltage-activated K^+ channels using whole-cell patch clamp recordings (Fig. 2). We have, therefore, investigated the depolarization-evoked, K^+ currents in these four, electrophysiological subtypes of neurons using whole-cell patch clamp recordings.

Firing phenotype and intrinsic properties were first examined using the current-clamp configuration (Fig. 2, Upper row). Neurons were classified as slow firing (n=6), regular firing (n=4), fast spiking (n=6) and burst firing (n=5) according to criteria described

elsewhere (Henderson et al., 2001). An analysis of the intrinsic properties of the recorded neurons is presented in Table 1. As described for slow firing neurons, the width and slope of decay of the action potential significantly larger than the other neuronal subtypes (ANOVA, $P<0.05$, Tukey's HSD post-hoc analysis, $P<0.05$, Table 1). These neurons also exhibited the lower steady-state firing frequency (10.5±3.5 Hz) when compared to regular firing (24.1±5.3 Hz), fast spiking (42.2±7.8 Hz) and burst-firing neurons (38.5±5.1 Hz) after ANOVA statistical and Tukey's HSD post-hoc analyses ($P<0.05$).

After determining the intrinsic properties, depolarization-activated outward currents were studied under voltage-clamp configuration in a solution that blocked voltage-gated Na^+ and Ca^{2+} currents. Two major components of the voltage-gated K^+ currents were examined using specific voltage steps and subtraction protocols (Figure 1). Representative voltage-activated K^+ currents recorded in these different electrophysiological phenotypes revealed striking difference, specifically in the rapidly activating and rapidly inactivating currents, termed A-type transient current (I_A) (Fig. 2). The amplitude and activation kinetics of I_A varied among MS/DB neurons (Figure 2, Table 2). Distinctively, slow firing neurons exhibited the larger amplitude (current peak) and density of I_K and I_A when compared to other neuronal subtypes (ANOVA and Tukey's HSD, $P<0.05$, Table 2). The threshold and activation curve midpoint for I_A was significantly lower (at more hyperpolarized potentials) in slow firing neurons (Figure 2, Table 2). Moreover, the I_K activation curve midpoint and steepness were significantly higher in this group. Fast spiking and burst firing neurons exhibited a lower density of I_A currents (91.0±26 pA/pF and 109.1±11.49pA/pF respectively) and a higher threshold of activation (−31.4±2.6 mV and −37.5±2.5) (Table 2). The variability in I_K and I_A density, waveforms and activation kinetics indicate that MS/DB neurons exhibit a differential subset of voltage-gated K^+ channels and that I_A is a predominant current in slow firing neurons.

To further explore this notion of voltage-gated K^+ current variability, we investigated the pharmacological sensitivity of K^+ currents to the K^+ channel blockers 4-AP on TEA in MS/DB neurons. Baseline outward currents (control) were recorded prior to superfusion of the 4-AP-contaning ACSF solution. Pharmacological actions were measured when the effect of each concentration of 4-AP had reached steady-state. In these experiments, the effects of increasing concentrations (0.1, 0.5, 1, 10, 20 mM) of 4-AP on K^+ currents in MS/DB neurons were examined (Figure 3 A2, B2, C2, D2). These experiments demonstrate that 4-AP inhibits I_A in a concentration-dependent manner; therefore, remaining K^+ currents were challenged with a co-application of 20 mM 4-AP and 20mM TEA (Figure 3, A3–D3).

To analyze the current inhibited by different concentrations of 4-AP, current traces recorded in the presence of each concentration of 4-AP were digitally subtracted from the control traces (in the absence of 4-AP). As evident in Figure 3 A3, the current blocked by 0.1 mM and 0.5 mM of 4-AP activates rapidly and inactivates rapidly as I_A in slow firing neurons (Figure 3A) and regular firing neurons (Figure 3B). Fast spiking and burst firing neurons exhibited small, transient, A-type currents. These transient components were less sensitive to 4-AP with a IC50 of 2.5 mM in fast spiking (Figure 3, C4) and 1.3 mM in bust firing neurons (Figure 3, D4). As previously reported, 4-AP had a minimal effect on the slowly inactivating outward current, reducing the total current to approximately 80% of control at 10 mM 4-AP. The slowly inactivating component was successfully blocked in all experiments by 20 mM TEA (Figure 3, A2-D2, A3-D3). These pharmacological experiments confirm that, in contrast to slow firing and regular firing neurons, fast spiking and burst firing neurons in the MS/DB express a minimal amount of I_A.

Next, we investigated the sensitivity of action potential width and latency to 4-AP in different neuronal phenotypes. pplication of 100 μM 4-AP significantly reduced the latency

of the first action potential in slow firing and regular firing neurons but failed to significantly modify these variables in fast spiking and bursting firing neurons (Figure 4, A1-D1). Application of 4-AP (100 μM) significantly increased the width of action potential in slow firing (40.5±5.6% increase, paired Student t-test, $p<0.01$) and regular firing neurons (18.1±4.5% increase, paired Student t-test<0.05). However, significant changes were not detected in fast spiking and burst firing neurons (Figure 4, A2–D2). In addition, 4-AP increased firing frequency in all neuronal subtypes, but the effect was more evident in slow firing neurons (Figure 4).

DISCUSSION

The operation of neuronal networks depends on the firing patterns of the interconnected neurons. The firing patterns and input-output functions of network's neurons are determined by their intrinsic electrophysiological properties which in turn can influence the emerging functional properties of the network. Previous studies indicate that K^+ currents control different features of firing patterns in neurons (Connor and Stevens, 1971a; Yarom et al., 1985). As an example, I_K affects the action potential waveform while I_A changes firing rates in rat suprachiasmatic neurons (Bouskila and Dudek, 1995). I_M widely regulates neuronal excitability in brain structures; in hippocampal pyramidal neurons I_M facilitates repetitive discharges, enhances after-depolarization and burst-firing, and induces spontaneous firing through a reduction of action potential threshold at the axon initial segment (Brown and Passmore, 2009). As a result, the expression of K^+ channels can shape firing patterns and modulate neuronal excitability. These K^+ channel functions may play an important role in determining intrinsic properties of basal forebrain networks (including septal neurons) that provide extensive innervations to neocortical and archicortical structures, controlling their excitability and rhythmic processes.

It is possible that firing patterns in MS/DB neuronal subtypes are determined by interplay of different ionic conductances including K^+ currents. Although this study investigates differences in voltage-gated I_K and I_A currents we cannot rule out that firing phenotypes are determined by a more complex interaction and differential expression of Ca^{2+}-activated K^+ current, voltage-gated Na^+ and Ca^{2+} currents. In support of this notion, a previous study demonstrates that transient, high-threshold Ca^{2+}, and apamin-sensitive Ca^{2+}-activated K^+ conductancse are responsible for the generation of slow afterhyperpolarizing potential (sAHP) which has been implicated in limiting the firing rate (*e.g.* slow firing) in MS/DB cholinergic neurons (Gorelova and Reiner, 1996). Application of K^+ current blocker 4-AP (preferentially I_A) increased the firing frequency of slow firing neurons while a less pronounced effect was detected on regular, fast and burst-firing neurons. These findings indicate that under normal conditions, voltage-dependent activation of I_A may also control firing frequency in slow firing neurons. It is possible that when activated by depolarizing currents or during an action potential the large amplitude I_A on slow firing neurons may provoke prominent hyperpolarization of the membrane reducing the probability for subsequent generation of action potentials. It has been proposed that activation of I_A at subthreshold potentials can contribute to delayed firing of action potentials during slow approaches to threshold (Connor and Stevens, 1971a, b; Segal and Barker, 1984; Segal et al., 1984; Storm, 1988) Consequentially, pronounced I_A may interplay with other conductances to determine longer inter-spike intervals in slow firing neurons. Since voltage- and calcium-activated potassium currents may be also responsible for slowing firing rates in these neurons, additional molecular and electrophysiological studies are necessary to investigate the roles of these currents in determining firing phenotypes in MS/DB neurons. In the septo-hippocampal system, the septal output influences synaptic plasticity in hippocampal networks (Frey et al., 2003). Thus, understanding the role of ionic conductances underlying

the firing patterns of septal neurons is relevant to elucidate septo-hippocampal functions (including theta rhythm generation) and dysfunction.

Heterogeneity in firing properties has been previously noted in MS/DB neurons (Garrido-Sanabria et al., 2007a; Griffith and Matthews, 1986; Knapp et al., 2000; Manseau et al., 2008; Morris and Henderson, 2000; Simon et al., 2006; Sotty et al., 2003). Our data indicate that these distinct intrinsic firing phenotypes are associated with the expression of specific K^+ currents among MS/DB neurons. Slow firing and regular firing neurons expressed prominent I_A while fast spiking and bursting neurons exhibited mostly delayer rectifier K^+ currents with only minimal contributions of the I_A.

A-type, K^+ channels are prominent in the somatodendritic membrane of mammalian neurons (Bailey et al., 2007; Debanne et al., 1997; Huang et al., 2005; Jerng et al., 2004; Kollo et al., 2006; Menegola et al., 2008; Serodio and Rudy, 1998; Song et al., 1998; Tkatch et al., 2000; Tsaur et al., 2001). A-type, K^+ currents play an important role in the regulation of repetitive firing and synaptic integration. Therefore, differential expression of this current may determine the diversity of firing behavior in MS/DB neurons. For example, slow firing neurons are distinguished by long latency to first spike, evoked by threshold depolarizing steps, and very low firing rates. Expression of a large A-type current is consistent with a delayed firing onset in the presence of background hyperpolarization as observed in slow firing neurons. It has previously been suggested that such electrophysiological feature are governed by an inactivating, transient, A-type, K^+ current (Connor and Stevens, 1971a) . Consistent with these data, slow firing neurons expressed significantly larger I_K and I_A current densities. Moreover, I_A are activated at a subthreshold membrane potential, which is in agreement with previous data showing that latency to first spike increases if slow firing neurons are hyperpolarized prior to depolarizing steps (Garrido-Sanabria et al., 2007a). Moreover, it has been largely demonstrated that MS/DB, slow firing neurons express a predominant, cholinergic, neurochemical phenotype (Garrido-Sanabria et al., 2007a; Gorelova and Reiner, 1996; Matthews and Lee, 1991; Sotty et al., 2003). Thus, discerning the molecular substrate/subunit composition of this I_A may provide an important target for the creation of agents that improve cognition in age-related disorders.

However, the subunits associated with I_A currents in MS/DB cholinergic or slow firing neurons have yet to be characterized. Previously, single-cell reverse transcription-PCR and patch clamp analyses revealed that cholinergic neostriatal inteneurons exhibit a low-frequency firing mediated via an A-type, K^+ current (Kv4.2 and Kv4.1 channels) (Serodio and Rudy, 1998; Song et al., 1998). Moreover, Kv4.2 mRNA abundance was linearly related to A-type, K^+ current amplitude in neostriatal, medium spiny neurons and cholinergic interneurons in globos pallidus and basal forebrain, cholinergic neurons (Tkatch et al., 2000).

In this study, there was not a significant correlation between estimates of Kv4.1 or Kv4.3 mRNA abundances and I_A K^+ current amplitude. In neostriatal neurons, selective blocks of I_A substantially decreased the latency to discharge and increased the frequency (Gabel and Nisenbaum, 1998). In agreement with these data, a block of I_A with 4-AP substantially increased the firing frequency in slow firing MS/DB neurons. I_A sensitivity to 4-AP suggests that the Kv4.2 and Kv4.3 channels' subunits may be substrates of I_A in slow firing medial septal neurons (Angelova and Muller, 2009; Wang and Schreurs, 2006). Molecular studies will be necessary to determine the molecular composition of K^+ channels mediating I_A in slow firing, MS/DB neurons.

Delayed rectifiers, K^+ currents are often attributable to the Kv2 and Kv3 subfamily genes. In a previous study, we reported that basal forebrain, cholinergic neurons express both Kv3.1

and Kv2.1 subunits (Betancourt and Colom, 2000). However, the Kv2.1 subunit showed a wider distribution in noncholinergic neurons than the Kv3.1 subunit. Kv3.1 and Kv2.1 immunostaining was noticeable not only in neuronal cell bodies but also in the dendritic ramifications of these neurons. Interestingly, the Kv3.1 subunit has been classically associated with fast-spiking neurons whereas basal forebrain, cholinergic neurons are characterized by slow firing frequency and long-duration action potentials (Betancourt and Colom, 2000). Thus, it appears that mammalian neurons express some particular Kv genes at higher levels while coexpressing multiple genes for the composition of depolarization-activated, K^+ channels (Song, 2002). The Kv3.1 subunits may have functions other than facilitating high-frequency firing in slow firing neurons. They may be responsible for slowly inactivating K^+ currents that are detected in slow firing neurons.

Since different types of K^+ channels influence the resting potential, firing threshold, spike depolarization and repetitive firing frequency (Connor & Stevens, 1971; Llinas, 1988, Koh et al., 1992; Safronov et al., 1996; Hille , 2001), their block or modulation may considerably affect neuronal excitability and the generation of firing patterns. As a result, this can modify the rhythmic activity in areas such as the MS/DB. Accordingly, K^+ channels' modulators have been considered an important therapeutic alternative in several neurological disorders (Alkon, 1999; Benatar, 2000; Kanai et al., 2006; Wulff et al., 2009; Wulff and Zhorov, 2008).

In conclusion, the four firing phenotypes of medial septal neurons show major differences in K^+ channel expression with the septal slow-firing neurons displaying the largest K^+ currents and a particularly prominent I_A. The discernment of the channels' subunits underlying these currents eit is particularly relevant for the ongoing age-related research. The identification of molecular targets with the subsequent modulation of these currents provides an exciting tool to enhance memory and learning processes in the elderly.

Acknowledgments

This work was supported by the following NIH grant: 3SC1NS065386-02S1 (NINDS/NIGMS) to L.V.C. E.R.G.S was also supported by P20MD001091 (NIH/NCMHD), 5SC1NS063950-04 (NIH/NIGMS/MBRS) and 3SC1NS063950-03S1 ARRA (NINDS/NIGMS).

References

Alkon DL. Ionic conductance determinants of synaptic memory nets and their implications for Alzheimer's disease. J Neurosci Res. 1999; 58:24–32. [PubMed: 10491569]

Andersen P, Bland HB, Myhrer T, Schwartzkroin PA. Septo-hippocampal pathway necessary for dentate theta production. Brain Res. 1979; 165:13–22. [PubMed: 427577]

Angelova PR, Muller WS. Arachidonic acid potently inhibits both postsynaptic-type Kv4.2 and presynaptic-type Kv1.4 IA potassium channels. Eur J Neurosci. 2009; 29:1943–1950. [PubMed: 19453640]

Angulo E, Noe V, Casado V, Mallol J, Gomez-Isla T, Lluis C, Ferrer I, Ciudad CJ, Franco R. Up-regulation of the Kv3.4 potassium channel subunit in early stages of Alzheimer's disease. J Neurochem. 2004; 91:547–557. [PubMed: 15485486]

Bailey TW, Hermes SM, Whittier KL, Aicher SA, Andresen MC. A-type potassium channels differentially tune afferent pathways from rat solitary tract nucleus to caudal ventrolateral medulla or paraventricular hypothalamus. J Physiol. 2007; 582:613–628. [PubMed: 17510187]

Benatar M. Neurological potassium channelopathies. QJM. 2000; 93:787–797. [PubMed: 11110585]

Betancourt L, Colom LV. Potassium (K+) channel expression in basal forebrain cholinergic neurons. J Neurosci Res. 2000; 61:646–651. [PubMed: 10972961]

Bland BH, Oddie SD. Theta band oscillation and synchrony in the hippocampal formation and associated structures: the case for its role in sensorimotor integration. Behav Brain Res. 2001; 127:119–136. [PubMed: 11718888]

Bland BH, Oddie SD, Colom LV. Mechanisms of neural synchrony in the septohippocampal pathways underlying hippocampal theta generation. J Neurosci. 1999; 19:3223–3237. [PubMed: 10191335]

Bland SK, Bland BH. Medial septal modulation of hippocampal theta cell discharges. Brain Res. 1986; 375:102–116. [PubMed: 3719349]

Bouskila Y, Dudek FE. A rapidly activating type of outward rectifier K+ current and A-current in rat suprachiasmatic nucleus neurones. J Physiol. 1995; 488 (Pt 2):339–350. [PubMed: 8568674]

Brauer K, Seeger G, Hartig W, Rossner S, Poethke R, Kacza J, Schliebs R, Bruckner G, Bigl V. Electron microscopic evidence for a cholinergic innervation of GABAergic parvalbumin-immunoreactive neurons in the rat medial septum. J Neurosci Res. 1998; 54:248–253. [PubMed: 9788283]

Brown DA, Passmore GM. Neural KCNQ (Kv7) channels. Br J Pharmacol. 2009; 156:1185–1195. [PubMed: 19298256]

Coetzee WA, Amarillo Y, Chiu J, Chow A, Lau D, McCormack T, Moreno H, Nadal MS, Ozaita A, Pountney D, Saganich M, Vega-Saenz de Miera E, Rudy B. Molecular diversity of K+ channels. Ann N Y Acad Sci. 1999; 868:233–285. [PubMed: 10414301]

Colom LV, Diaz ME, Beers DR, Neely A, Xie WJ, Appel SH. Role of potassium channels in amyloid-induced cell death. J Neurochem. 1998; 70:1925–1934. [PubMed: 9572276]

Connor JA, Stevens CF. Prediction of repetitive firing behaviour from voltage clamp data on an isolated neurone soma. J Physiol. 1971a; 213:31–53. [PubMed: 5575343]

Connor JA, Stevens CF. Voltage clamp studies of a transient outward membrane current in gastropod neural somata. J Physiol. 1971b; 213:21–30. [PubMed: 5575340]

Debanne D, Guerineau NC, Gahwiler BH, Thompson SM. Action-potential propagation gated by an axonal I(A)-like K+ conductance in hippocampus. Nature. 1997; 389:286–289. [PubMed: 9305843]

Freund TF. GABAergic septohippocampal neurons contain parvalbumin. Brain Res. 1989; 478:375–381. [PubMed: 2924136]

Frey S, Bergado JA, Frey JU. Modulation of late phases of long-term potentiation in rat dentate gyrus by stimulation of the medial septum. Neuroscience. 2003; 118:1055–1062. [PubMed: 12732250]

Gabel LA, Nisenbaum ES. Biophysical characterization and functional consequences of a slowly inactivating potassium current in neostriatal neurons. J Neurophysiol. 1998; 79:1989–2002. [PubMed: 9535963]

Garrido-Sanabria ER, Perez MG, Banuelos C, Reyna T, Hernandez S, Castaneda MT, Colom LV. Electrophysiological and morphological heterogeneity of slow firing neurons in medial septal/diagonal band complex as revealed by cluster analysis. Neuroscience. 2007a; 146:931–945. [PubMed: 17412516]

Garrido-Sanabria ER, Perez MG, Banuelos C, Reyna T, Hernandez S, Castaneda MT, Colom LV. Electrophysiological and morphological heterogeneity of slow firing neurons in medial septal/diagonal band complex as revealed by cluster analysis. Neuroscience. 2007b

Geula C. Abnormalities of neural circuitry in Alzheimer's disease: hippocampus and cortical cholinergic innervation. Neurology. 1998; 51:S18–29. discussion S65-17. [PubMed: 9674759]

Gorelova N, Reiner PB. Role of the afterhyperpolarization in control of discharge properties of septal cholinergic neurons in vitro. J Neurophysiol. 1996; 75:695–706. [PubMed: 8714645]

Griffith WH. Membrane properties of cell types within guinea pig basal forebrain nuclei in vitro. J Neurophysiol. 1988; 59:1590–1612. [PubMed: 3385475]

Griffith WH, Matthews RT. Electrophysiology of AChE-positive neurons in basal forebrain slices. Neurosci Lett. 1986; 71:169–174. [PubMed: 3785743]

Hall AM, Moore RY, Lopez OL, Kuller L, Becker JT. Basal forebrain atrophy is a presymptomatic marker for Alzheimer's disease. Alzheimers Dement. 2008; 4:271–279. [PubMed: 18631978]

Henderson Z, Lu CB, Janzso G, Matto N, McKinley CE, Yanagawa Y, Halasy K. Distribution and role of Kv3.1b in neurons in the medial septum diagonal band complex. Neuroscience. 2010; 166:952–969. [PubMed: 20083165]

Henderson Z, Morris NP, Grimwood P, Fiddler G, Yang HW, Appenteng K. Morphology of local axon collaterals of electrophysiologically characterised neurons in the rat medial septal/diagonal band complex. J Comp Neurol. 2001; 430:410–432. [PubMed: 11169477]

Hernandez-Pineda R, Chow A, Amarillo Y, Moreno H, Saganich M, Vega-Saenz de Miera EC, Hernandez-Cruz A, Rudy B. Kv3.1–Kv3.2 channels underlie a high-voltage-activating component of the delayed rectifier K+ current in projecting neurons from the globus pallidus. J Neurophysiol. 1999; 82:1512–1528. [PubMed: 10482766]

Huang HY, Cheng JK, Shih YH, Chen PH, Wang CL, Tsaur ML. Expression of A-type K channel alpha subunits Kv 4.2 and Kv 4.3 in rat spinal lamina II excitatory interneurons and colocalization with pain-modulating molecules. Eur J Neurosci. 2005; 22:1149–1157. [PubMed: 16176357]

Jackson J, Bland BH. Medial septal modulation of the ascending brainstem hippocampal synchronizing pathways in the anesthetized rat. Hippocampus. 2006; 16:1–10. [PubMed: 16270322]

Jerng HH, Pfaffinger PJ, Covarrubias M. Molecular physiology and modulation of somatodendritic A-type potassium channels. Mol Cell Neurosci. 2004; 27:343–369. [PubMed: 15555915]

Kanai K, Kuwabara S, Misawa S, Tamura N, Ogawara K, Nakata M, Sawai S, Hattori T, Bostock H. Altered axonal excitability properties in amyotrophic lateral sclerosis: impaired potassium channel function related to disease stage. Brain. 2006; 129:953–962. [PubMed: 16467388]

Kerrigan TL, Atkinson L, Peers C, Pearson HA. Modulation of 'A'-type K+ current by rodent and human forms of amyloid beta protein. Neuroreport. 2008; 19:839–843. [PubMed: 18463498]

Kidd JF, Brown LA, Sattelle DB. Effects of amyloid peptides on A-type K+ currents of Drosophila larval cholinergic neurons. J Neurobiol. 2006; 66:476–487. [PubMed: 16470685]

Kidd JF, Sattelle DB. The effects of amyloid peptides on A-type K(+) currents of Drosophila larval cholinergic neurons: modeled actions on firing properties. Invert Neurosci. 2006; 6:207–213. [PubMed: 17106756]

Kiss J, Patel AJ, Freund TF. Distribution of septohippocampal neurons containing parvalbumin or choline acetyltransferase in the rat brain. J Comp Neurol. 1990; 298:362–372. [PubMed: 2212109]

Knapp JA, Morris NP, Henderson Z, Matthews RT. Electrophysiological characteristics of non-bursting, glutamate decarboxylase messenger RNA-positive neurons of the medial septum/diagonal band nuclei of guinea-pig and rat. Neuroscience. 2000; 98:661–668. [PubMed: 10891609]

Kollo M, Holderith NB, Nusser Z. Novel subcellular distribution pattern of Atype K+ channels on neuronal surface. J Neurosci. 2006; 26:2684–2691. [PubMed: 16525047]

Lawson VH, Bland BH. The role of the septohippocampal pathway in the regulation of hippocampal field activity and behavior: analysis by the intraseptal microinfusion of carbachol, atropine, and procaine. Exp Neurol. 1993; 120:132–144. [PubMed: 8477826]

Li Y, Um SY, McDonald TV. Voltage-gated potassium channels: regulation by accessory subunits. Neuroscientist. 2006; 12:199–210. [PubMed: 16684966]

Manseau F, Goutagny R, Danik M, Williams S. The hippocamposeptal pathway generates rhythmic firing of GABAergic neurons in the medial septum and diagonal bands: an investigation using a complete septohippocampal preparation in vitro. J Neurosci. 2008; 28:4096–4107. [PubMed: 18400909]

Matthews RT, Lee WL. A comparison of extracellular and intracellular recordings from medial septum/diagonal band neurons in vitro. Neuroscience. 1991; 42:451–462. [PubMed: 1680227]

Menegola M, Misonou H, Vacher H, Trimmer JS. Dendritic A-type potassium channel subunit expression in CA1 hippocampal interneurons. Neuroscience. 2008; 154:953–964. [PubMed: 18495361]

Morris NP, Harris SJ, Henderson Z. Parvalbumin-immunoreactive, fast-spiking neurons in the medial septum/diagonal band complex of the rat: intracellular recordings in vitro. Neuroscience. 1999; 92:589–600. [PubMed: 10408608]

Morris NP, Henderson Z. Perineuronal nets ensheath fast spiking, parvalbumin-immunoreactive neurons in the medial septum/diagonal band complex. Eur J Neurosci. 2000; 12:828–838. [PubMed: 10762312]

Pannaccione A, Boscia F, Scorziello A, Adornetto A, Castaldo P, Sirabella R, Taglialatela M, Di Renzo GF, Annunziato L. Up-regulation and increased activity of KV3.4 channels and their accessory subunit MinK-related peptide 2 induced by amyloid peptide are involved in apoptotic neuronal death. Mol Pharmacol. 2007; 72:665–673. [PubMed: 17495071]

Peusner KD, Gamkrelidze G, Giaume C. Potassium currents and excitability in second-order auditory and vestibular neurons. J Neurosci Res. 1998; 53:511–520. [PubMed: 9726422]

Plant LD, Webster NJ, Boyle JP, Ramsden M, Freir DB, Peers C, Pearson HA. Amyloid beta peptide as a physiological modulator of neuronal 'A'-type K+ current. Neurobiol Aging. 2006; 27:1673–1683. [PubMed: 16271805]

Rudy B. Molecular diversity of ion channels and cell function. Ann N Y Acad Sci. 1999; 868:1–12. [PubMed: 10414277]

Schliebs R, Arendt T. The significance of the cholinergic system in the brain during aging and in Alzheimer's disease. J Neural Transm. 2006; 113:1625–1644. [PubMed: 17039298]

Schwindt PC, Spain WJ, Foehring RC, Stafstrom CE, Chubb MC, Crill WE. Multiple potassium conductances and their functions in neurons from cat sensorimotor cortex in vitro. J Neurophysiol. 1988; 59:424–449. [PubMed: 3351569]

Segal M, Barker JL. Rat hippocampal neurons in culture: potassium conductances. J Neurophysiol. 1984; 51:1409–1433. [PubMed: 6330315]

Segal M, Rogawski MA, Barker JL. A transient potassium conductance regulates the excitability of cultured hippocampal and spinal neurons. J Neurosci. 1984; 4:604–609. [PubMed: 6699688]

Serafin M, Williams S, Khateb A, Fort P, Muhlethaler M. Rhythmic firing of medial septum non-cholinergic neurons. Neuroscience. 1996; 75:671–675. [PubMed: 8951863]

Serodio P, Rudy B. Differential expression of Kv4 K+ channel subunits mediating subthreshold transient K+ (A-type) currents in rat brain. J Neurophysiol. 1998; 79:1081–1091. [PubMed: 9463463]

Simon AP, Poindessous-Jazat F, Dutar P, Epelbaum J, Bassant MH. Firing properties of anatomically identified neurons in the medial septum of anesthetized and unanesthetized restrained rats. J Neurosci. 2006; 26:9038–9046. [PubMed: 16943562]

Song WJ. Genes responsible for native depolarization-activated K+ currents in neurons. Neurosci Res. 2002; 42:7–14. [PubMed: 11814604]

Song WJ, Tkatch T, Baranauskas G, Ichinohe N, Kitai ST, Surmeier DJ. Somatodendritic depolarization-activated potassium currents in rat neostriatal cholinergic interneurons are predominantly of the A type and attributable to coexpression of Kv4.2 and Kv4.1 subunits. J Neurosci. 1998; 18:3124–3137. [PubMed: 9547221]

Sotty F, Danik M, Manseau F, Laplante F, Quirion R, Williams S. Distinct electrophysiological properties of glutamatergic, cholinergic and GABAergic rat septohippocampal neurons: novel implications for hippocampal rhythmicity. J Physiol. 2003; 551:927–943. [PubMed: 12865506]

Storm JF. Temporal integration by a slowly inactivating K+ current in hippocampal neurons. Nature. 1988; 336:379–381. [PubMed: 3194020]

Stucky CL, Lewin GR. Isolectin B(4)-positive and -negative nociceptors are functionally distinct. J Neurosci. 1999; 19:6497–6505. [PubMed: 10414978]

Tkatch T, Baranauskas G, Surmeier DJ. Kv4.2 mRNA abundance and A-type K(+) current amplitude are linearly related in basal ganglia and basal forebrain neurons. J Neurosci. 2000; 20:579–588. [PubMed: 10632587]

Traub RD, Wong RK, Miles R, Michelson H. A model of a CA3 hippocampal pyramidal neuron incorporating voltage-clamp data on intrinsic conductances. J Neurophysiol. 1991; 66:635–650. [PubMed: 1663538]

Tsaur ML, Wu YL, Huang FL, Shih YH. Localization of A-type K+ channel subunit Kv4.2 in rat brain. Chin J Physiol. 2001; 44:133–142. [PubMed: 11767285]

Wang D, Schreurs BG. Characteristics of IA currents in adult rabbit cerebellar Purkinje cells. Brain Res. 2006; 1096:85–96. [PubMed: 16716270]

Wu M, Newton SS, Atkins JB, Xu C, Duman RS, Alreja M. Acetylcholinesterase inhibitors activate septohippocampal GABAergic neurons via muscarinic but not nicotinic receptors. J Pharmacol Exp Ther. 2003; 307:535–543. [PubMed: 12966162]

Wulff H, Castle NA, Pardo LA. Voltage-gated potassium channels as therapeutic targets. Nat Rev Drug Discov. 2009; 8:982–1001. [PubMed: 19949402]

Wulff H, Zhorov BS. K+ channel modulators for the treatment of neurological disorders and autoimmune diseases. Chem Rev. 2008; 108:1744–1773. [PubMed: 18476673]

Yarom Y, Sugimori M, Llinas R. Ionic currents and firing patterns of mammalian vagal motoneurons in vitro. Neuroscience. 1985; 16:719–737. [PubMed: 2419787]

Ye CP, Selkoe DJ, Hartley DM. Protofibrils of amyloid beta-protein inhibit specific K+ currents in neocortical cultures. Neurobiol Dis. 2003; 13:177–190. [PubMed: 12901832]

Yoder RM, Pang KC. Involvement of GABAergic and cholinergic medial septal neurons in hippocampal theta rhythm. Hippocampus. 2005; 15:381–392. [PubMed: 15630696]

Yu HB, Li ZB, Zhang HX, Wang XL. Role of potassium channels in Abeta(1–40)-activated apoptotic pathway in cultured cortical neurons. J Neurosci Res. 2006; 84:1475–1484. [PubMed: 17022037]

Research Highlights

- Slow firing neurons in medial septum exhibit large K^+ currents
- The type A current is the larger component of K+ currents in slow firing neurons
- Blockers of K^+ currents in slow firing neurons increase firing rate.

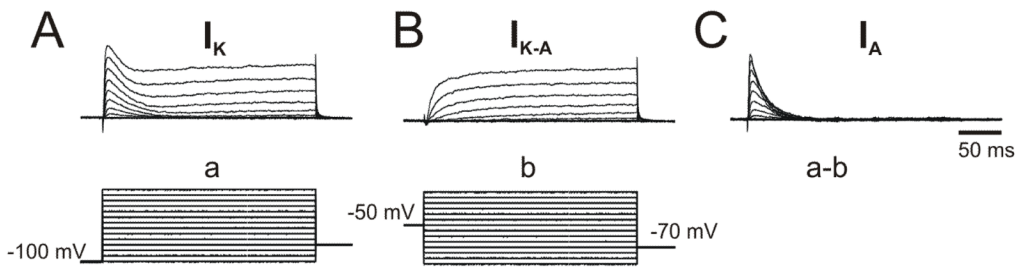

Figure 1.

Isolation of voltage-gated K^+ currents in different electrophysiological phenotypes of medial septal neurons. A. Recording of intrinsic neuronal properties was performed using current-clamp configuration. The whole-cell recording electrode was filled with a K^+, gluconate-based, internal solution. Hyperpolarizing and depolarizing square current pulses (400 msec duration) were injected (20 mV steps) to assess passive and active intrinsic properties of neurons. B. After analyzing the firing phenotype of the neurons, the recording configuration was switched to voltage-clamp to assess K^+ currents. The bathing solution was also changed to calcium-free ACSF containing 1 μM TTX (to block sodium currents) and 2 mM cobalt, a divalent cation to block calcium currents and calcium-activated currents. B1. Total voltage-gated K^+ currents (I_K) (a) were activated by a series of 400 msec incrementing voltage steps (10 mV steps) from a holding potential of −100 mV up to +60 mV. B2. The fast, transient, A-type, K^+ currents (I_A) are inactivated by prepulsing the neurons to −50 mV for 500 ms (b), resulting in the isolation of the delayer rectifier (I_K-I_A) component. B3. A family of I_A currents was evident after subtracting b from a as follows $I_A = I_K - (I_K\text{-}I_A)$ (a–b). In some experiments, I_A was isolated pharmacologically by adding 4-AP.

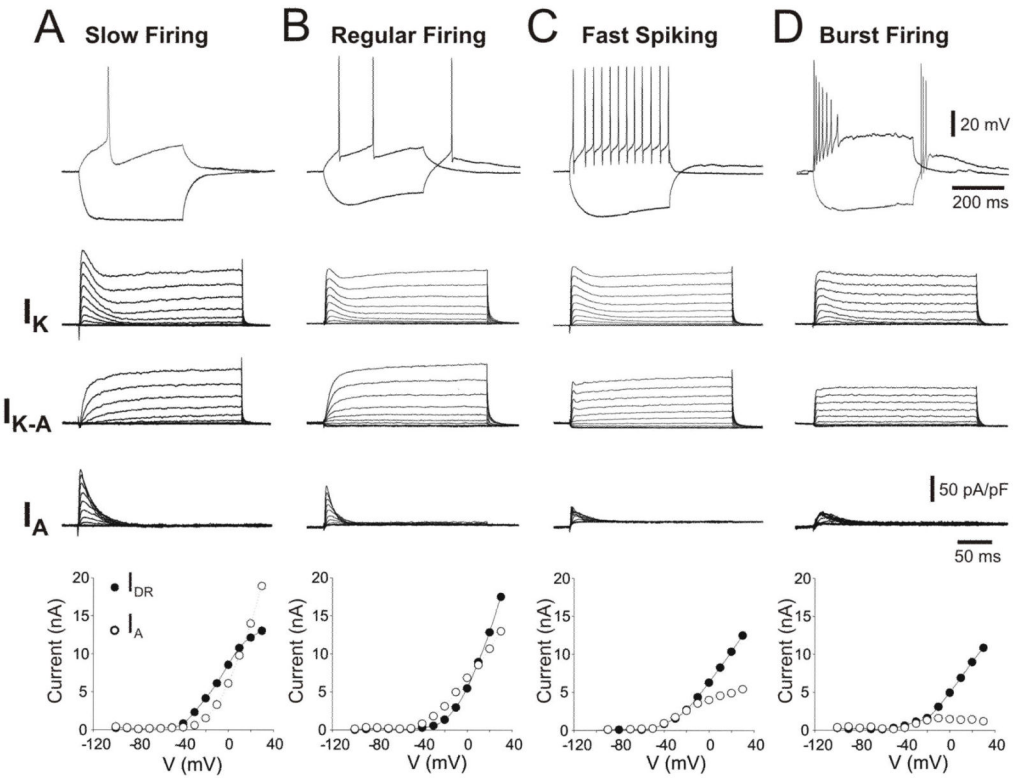

Figure 2.

The waveforms of calcium-independent, voltage-gated, K^+ currents (I_K, I_{DR} and I_A) (middle rows, represented as current densities) vary among the four main electrophysiological phenotypes (different intrinsic properties) observed in MS/DB neurons (top row). Note that (A) a representative slow firing neuron (exhibiting long latency for first action potential) and (B) regular firing neurons exhibited a more pronounced low-threshold I_A when compared to (C) fast spiking and (D) burst-firing neurons. This is evident in a plotted, voltage-current relationship for data averaged from several neurons per groups as indicated (n) (bottom row). The peak currents (components) at different voltage steps were detected and measured in the 10–50 msec interval for I_A (open circles) and from the 250–350 msec interval for I_{DR} (closed circles). Currents were evoked and detected as described in Figure 1.

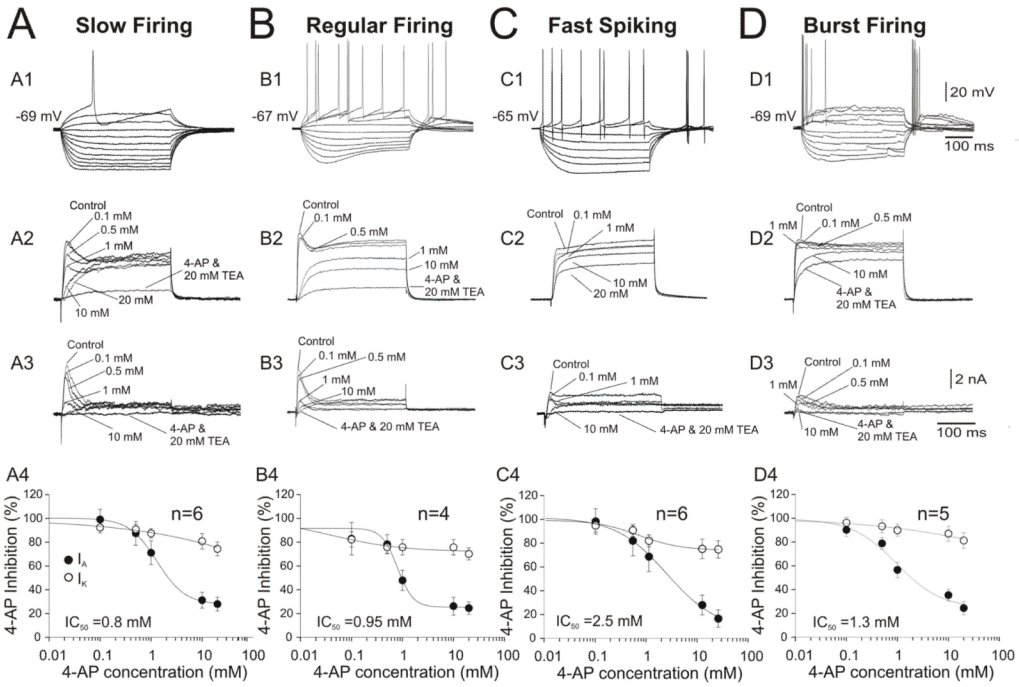

Figure 3.

The effect of external 4-AP and TEA on K^+ currents isolated from distinct neuronal phenotypes in the MS/DB area. (A.) The transient, A-type current component in a representative, slow firing neuron exhibiting no I_h and long latency for the first action potential (A1) was reduced by increasing concentrations of 4-AP (reaching ~10% after 1 mM 4-AP, IC_{50}=0.8 mM) (A4). The delayed rectifier (I_{DR}) component (plateau) was only reduced to 80% after 20 mM 4-AP but was attenuated up to 5% by TEA (20 mM) (A2–A4). (B.) A regular firing neuron with prominent I_h and rebound firing exhibited an I_A current less sensitive to low 4-AP concentration than I_A in slow firing neurons but with a similar range of IC_{50}=0.95 mM (B4). The I_{DR} component was also highly sensitive to TEA (20 mM) (B3) but not to 4-AP (B4). A representative fast spiking neuron (C1) exhibiting small I_A that is more resistant to 4-AP (IC_{50}=2.5 mM, C4), I_{DR} was also resistant (only 50%) bloc to TEA (C2). A representative bursting neuron expressing small I_A sensitive to 4-AP (IC_{50}=1.3 mM, C4). The plots of the normalized peak amplitude for I_A and I_K against the concentration of 4-AP were fitted by the sum of two logistic functions.

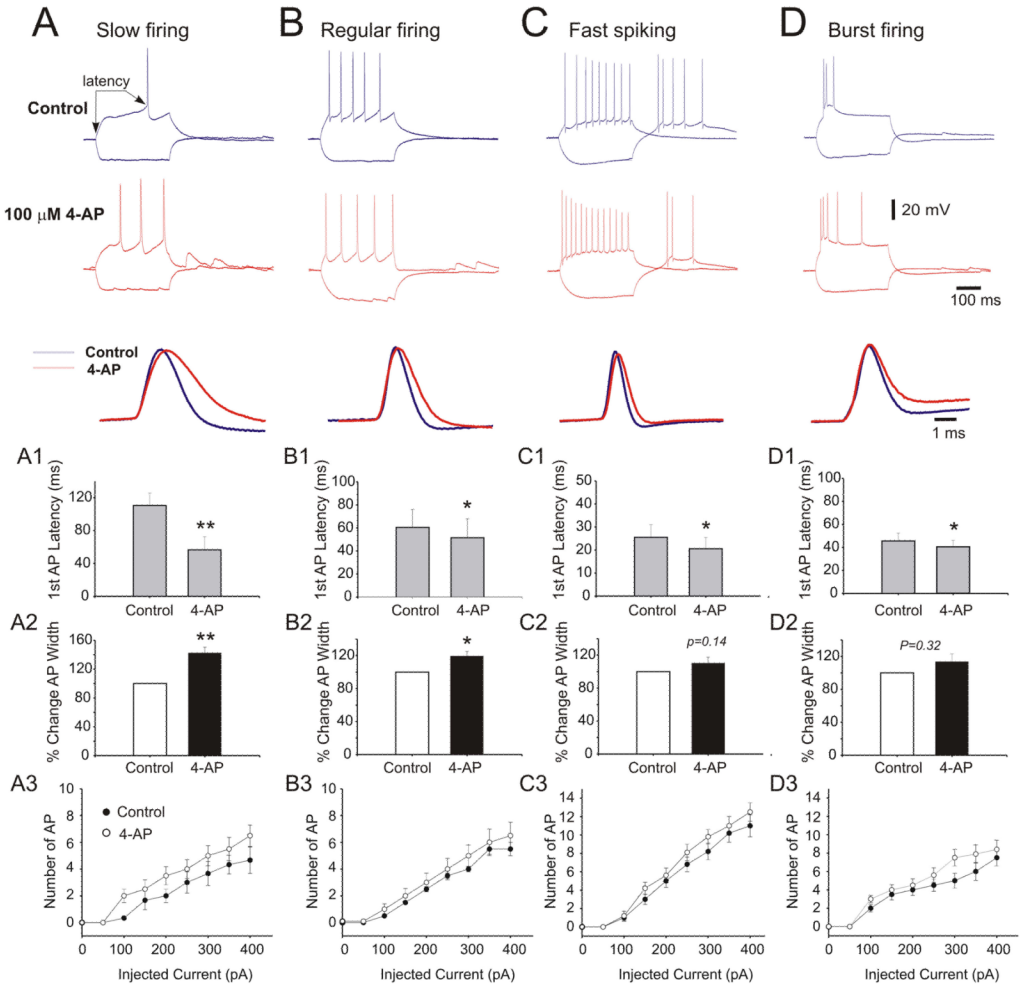

Figure 4.

4-aminopyridine (4-AP, 200 μM) impairs action potential (AP) repolarization and slows high-frequency firing of RGCs. (A) left panel shows repetitive firing of RGC under control conditions. Right panel shows the responses to identical currents in the presence of 200 μM 4-AP. 4-AP profoundly reduced the steady-state firing frequency for all intensities of stimulating currents, which are indicated above each pair of traces. The holding current was −210 pA. (B) 200 μM 4-AP caused AP broadening of a neuron by reducing the repolarization rate and suppressing afterhyperpolarization of single APs evoked by near-threshold depolarizations. Left panel shows the voltage waveform. Right panel shows the numerical time derivative of this waveform. IS-SD break is indicated by arrow. (A) and (B) are from different cells.

Table 1

Intrinsic membrane properties in MS/DB neuronal subtypes.

Properties	Slow firing	Fast-spiking	Regular-firing	Burst-firing	*P*
V_m (mV)	−67.2 ± 532	−69.5 ± 6.7	−68.6 ± 4.8	−71.1 ± 6.5	0.35
R_m (MΩ)	75.4 ± 5.3	90.7 ± 8.1	86.0 ± 6.8	94.2 ± 9.1	0.93
τ_m (ms)	36.6 ± 3.5	36.3 ± 2.8	45.0 ± 4.2	41.5 ± 3.5	0.30
AP threshold (mV)	49.9 ± 4.5	52.1 ± 4.2	52.3 ± 5.1	54.4 ± 4.8	0.22
AP half-width (ms)	2.2 ± 0.5	1.1 ± 0.3	1.2 ± 0.4	1.3 ± 0.3	.0001*
AP amplitude (mV)	84.9 ± 5.6	83.4 ± 8.5	84.2 ± 7.5	79.2 ± 6.2	0.55
AP rise slope (mV/ms)	64.7 ± 4.9	97.1 ± 6.5	73.2 ± 5.6	79.4 ± 5.2	0.63
AP decay slope (mV/ms)	−32.9 ± 3.1	−67.2 ± 2.9	−51.5 ± 3.7	−68.6 ± 4.3	.0020*
fAHP (mV)	−3.48 ± 0.4	−5.3 ± 0.7	−3.1 ± 0.5	−5.7 ± 0.9	.178

Recordings from MS/DB neurons with different firing patterns. V_m, resting membrane potential; R_m, input resistance; τ_m, membrane time constant; AP, action potential; ADP, after-depolarization; fAHP, fast after-hyperpolarizing potential. Values are expressed as means ± SEM, *P* statistical significance (One-way ANOVA analysis).

Table 2

Analysis of voltage-gated K^+ currents in MS/DB neurons.

I_K	Slow Firing n=6	Regular Firing n=4	Fast Firing n=6	Burst Firing n=5	*P*
I_K peak current (nA)	18.4±2.5*	13.5±3.5	8.61±2.8**	10.5±3.8	<0.05
I_K peak current density (pA/pF)	390.7±37.9*	341.28±62.9	312.4±73.5	337.8±58.2	0.7
Activation curve midpoint (mV)	17.02±3.8*	14.04±2.4	15.94±0.8	12.06±6.2	0.48
I_K Steepness,δ (pA/mV)	−7.4±1.1*	−4.06±0.7	−4.22±0.5	0.52±0.4*	<0.05
I_{DR} threshold (mV)	−44.28±3.6	−36.6±2.1	−37.5±2.5	−33.3±3.3	0.14
TEA IC_{50} (mM)	1.1	1.5	-	1.5	0.12
I_A					
I_A peak current (nA)	12.7±3.1*	5.8±2.6	5.0±1.8	5.6±2.8	<0.05
I_A peak current density (pA/pF)	211.64±37.9*	179.3±40.6	91.0±26*	109.1±11.49	<0.05
10–90% rise time (ms)	3.8±0.8*	3.1±0.7	1.4±0.2*	2.6±0.7	<0.05
Decay time constant (ms)	86.5±6.8*	42.5±6.7	28.5±8.2	31.5±5.7	<0.05
Activation curve midpoint (mV)	−28.3±3.7*	−15.68±4.4	−10.21±3.59	−10.9±3.5	<0.05
I_A Steepness,δ (pA/mV)	17.2±1.97	13.9±3.9	12.94±0.46	11.08±5.4	0.09
I_A threshold (mV)	−44.2±2.9*	−40.0±4.08	−31.4±2.6	−37.5±2.5	<0.05
4-AP IC_{50} (mM)	0.85	0.95	1.1	1.3	0.14
I_A/I_K ratio	0.58±0.1*	0.5±0.08*	0.38±0.21	0.35±0.1	<0.05

Data presented as mean ± standard deviation, *P* statistical significance (One-way ANOVA analysis).